J Radioanal Nucl Chem (2010) 284:367–375
DOI 10.1007/s10967-010-0522-8

Standardization of calibration procedures for quantification of gross alpha and gross beta activities using liquid scintillation counter

S. P. D. Bhade · P. J. Reddy · A. Narayanan · K. K. Narayan · D. A. R. Babu · D. N. Sharma

Received: 13 January 2010 / Published online: 26 March 2010

Abstract Simultaneous measurement of gross alpha and gross beta activities by liquid scintillation counting technique using LKB Wallac Quantulus 1220 liquid scintillation counter (LSC) equipped with Pulse Shape Analyzer (PSA) is described. Three sets of pure alpha and pure beta standards simulating the activity concentration values of real samples in terms of α/β activity ratios were used to calibrate the LSC. Calibration methodology for the Quantulus 1220 with respect to the above measurements using ^{241}Am and ^{90}Sr/^{90}Y standards of respective activity concentrations of $\sim$25 dpm and $\sim 10^4$ dpm is described in detail. Also highlighted the need to calibrate the LSC using another set of ^{241}Am and ^{90}Sr/^{90}Y standards of low and high activity concentrations respectively. The practicability and working performance of these calibration plots was checked by the validation trials with test samples spiked with ^{241}Am and ^{90}Sr/^{90}Y covering range of α/β activity ratios from 1:1 to 1:50.

Keywords Liquid scintillation counter (LSC) · Gross alpha and gross beta activities · Pulse shape analyzer (PSA) · ^{241}Am and ^{90}Sr/^{90}Y standards · α/β Activity ratio

Introduction

Liquid scintillation Counting is a well-established technique for the detection and quantitative measurement of soft as well as hard beta emitters. Simultaneous measurement of alpha and beta activities in liquid scintillation counters (LSC) based on pulse shape analysis (PSA) technique has been recognized for many years [1–3]. Unlike conventional LSCs where only particle energy in terms of pulse height is measured, when pulse shape is added as one more dimension, the energy spectrum turns into pulse height-pulse shape spectrum that enables alpha beta discrimination. Alpha and beta events in liquid scintillation cocktail are distinguished by examining the electronic pulses that are made up of prompt and delayed components. The difference between the delayed components of their fluorescent decay forms the basis for discrimination of alpha and beta pulses [4].

The purpose of this work was to standardize the calibration procedure for the discrimination of alpha/beta activities in a sample with minimum deviation (<10%) from the true activity levels and least variation from the optimized PSA setting.

Experimental

Activity measurements were performed with LKB Wallac Quantulus 1220 LSC equipped with Pulse Shape Analyzer (PSA), which enables the discrimination of alpha events from that of beta. In the present study, ^{241}Am (alpha energy (MeV)—5.49(85%) and 5.44 (12%)) and ^{90}Sr/^{90}Y (beta energy (MeV) −0.546(100%)/2.28(100%)) were used as an alpha and beta standards respectively [5]. Although in some studies on gross alpha beta analysis natural uranium and ^{226}Ra in equilibrium with its daughters were employed as alpha standards and ^{137}Cs and ^{90}Sr/^{90}Y were employed as beta standards [6], ^{241}Am and ^{90}Sr/^{90}Y standards were particularly chosen for the calibration studies as most of the

S. P. D. Bhade (✉) · P. J. Reddy · A. Narayanan · K. K. Narayan · D. A. R. Babu · D. N. Sharma
Radiation Safety Systems Division, Bhabha Atomic Research Centre, Mumbai 400085, India
e-mail: sonali@barc.gov.in

emitted alphas are in the energy range 4–6 meV, while the betas typically have E_{max} values below 2.5 meV. Moreover these standards remove uncertainty associated with in-growth of decay progeny and cover a useful energy range. ^{241}Am standard (0.2245 µCi/g) used in the present study was received from BIPM, France. ^{90}Sr/^{90}Y standard (15.54 µCi/g) procured from Board of Radiation and Isotope Technology (BRIT) was standardized by CIEMAT/NIST standardization technique to obtain absolute disintegration rate [7]. These standards were diluted with 0.1 N HCl and 0.1 N HNO_3 carrier solutions respectively.

Optimization of PSA setting

LKB Quantulus 1220 LSC incorporates two dual programmable Multi Channel Analyzers. This enables simultaneous measurement of four spectra, each with 1024 channel resolution. Setting the PSA level by means of user friendly software, it is possible to route alpha events into one half of the MCA (SP12) namely α-MCA and beta events into other half (SP11) namely β-MCA. Pulse shape analyzer has to be set for each and every sample to achieve the optimum separation of alpha events from that of beta. The optimum PSA level is a numeric parameter that is represented by a line, the angle of which is user controlled, divides the dual plane into short (beta) and long (alpha) pulse categories. When dividing line (PSA setting) is correctly set, counts from these two categories are stored as two separate spectra. The PSA levels can be scanned from 1 to 256 [2]. When NO PSA setting is used, all events are stored in α-MCA (SP12). As PSA values are scanned, some events from α-MCA start registering into the β-MCA. At an optimum PSA setting, alpha and beta events can be discriminated with minimum interference of beta events in α-MCA and alpha events in β-MCA.

Calibration procedure

Quantulus 1220 LSC was calibrated using pure ^{241}Am and ^{90}Sr/^{90}Y standard solutions of activity concentrations 11502 and 11098 dpm ($\alpha/\beta \sim 1$) respectively. For precise analysis of gross alpha and beta activities in low active samples (activity concentration <50 dpm), the LSC system was re-calibrated with another set of ^{241}Am and ^{90}Sr/^{90}Y standards with activity concentration 22.6 and 28 dpm respectively. Additionally pure ^{241}Am standard of 49.25 dpm and pure ^{90}Sr/^{90}Y standard of 930.7 dpm ($\alpha/\beta \sim 1{:}20$) were also used to calibrate LSC. At each calibration stage, the procedure followed was same as described by Sanchez-Cabeza, J.A [8].

PSA levels were scanned for ^{241}Am and ^{90}Sr/^{90}Y standards and the percentage interference for each PSA setting

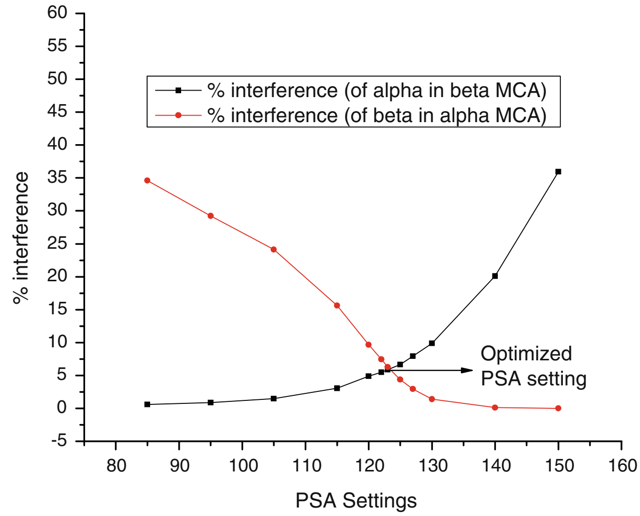

Fig. 1 Spillover plots of % interference of alpha events in beta MCA and beta events in alpha MCA corresponding to SQP(E)—812 for ^{241}Am and ^{90}Sr/^{90}Y standards of $\sim 10^4$ dpm

was calculated. When a pure ^{241}Am standard was counted, alpha interference was calculated as the fraction of counts observed in β-MCA (SP11) to the counts observed in α and β-MCA (SP12 + SP11). Similarly when a pure ^{90}Sr/^{90}Y source was counted, beta interference was calculated as the fraction of counts observed in α-MCA (SP12) to the counts observed in α and β-MCA (SP12 + SP11). A plot of percentage spillover against the PSA setting is illustrated in Fig. 1. The two spillover curves plotted are referred as crossover plots [9]. The PSA setting at which the two spillover curves cross was selected as optimized PSA setting for which minimum spillover of alpha events in β-MCA and beta events in α-MCA was observed.

It is a known fact that counting efficiencies and the optimized PSA settings are affected by the degree of quenching in the sample [5]. Quantification of quench level with respect to detection (E_α and E_β) and spillover ($E_{\alpha f}$ and $E_{\beta f}$) efficiencies of α and β radiation is accomplished by constructing quench curve using set of quenched standards. Amount of nitro methane added to the standard vials was sequentially increased from 0 to 0.25 mL representing Spectral Quench Parameter of External standard (SQP(E)) values in the range 905–540. This SQP(E) range covers the quench levels which are usually associated with the samples. PSA settings were optimized for various quench levels and plotted against subsequent SQP(E) values as illustrated in Figs. 2 and 3. Figure 2 displays the correlation between the external quench parameter SQP(E) and optimized PSA setting for Quicksafe-400 scintillation cocktail using ^{241}Am and ^{90}Sr/^{90}Y standards of respective activity concentrations $\sim 10^4$ dpm and ~ 25 dpm. Figure 3 illustrates the similar correlation for $L_\alpha H_\beta$ calibration.

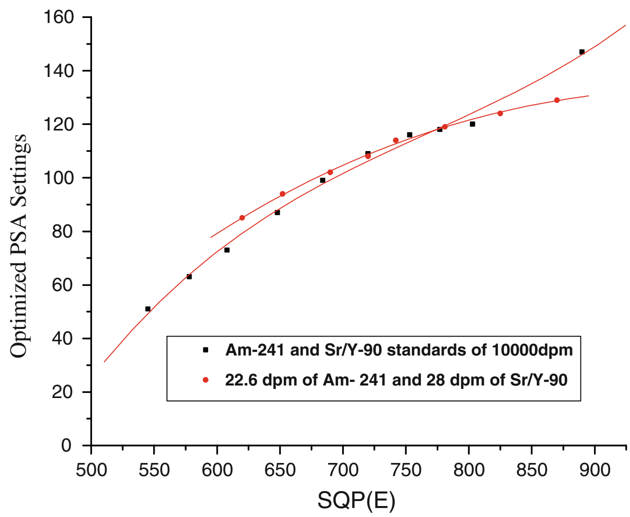

Fig. 2 Calibration plots prepared using ^{241}Am as an alpha standard and $^{90}Sr/^{90}Y$ as an beta standard, both having same activity concentrations $\sim 10^4$ dpm and $\sim$25 dpm in Quicksafe-400 scintillation cocktail with α/β activity ratio 1

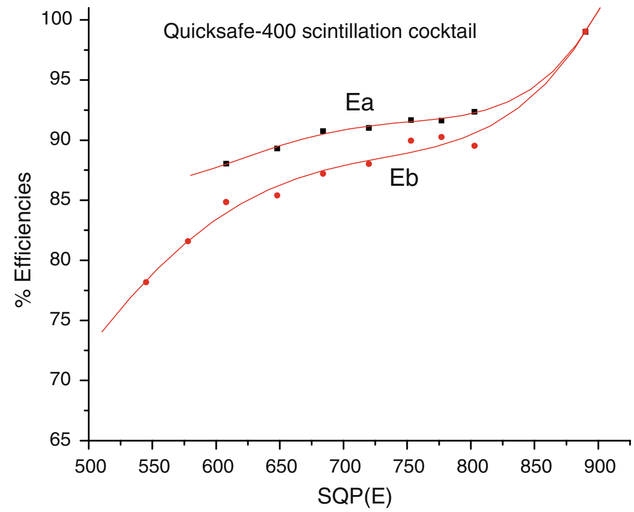

Fig. 4 Detection efficiencies plotted against SQP(E) for ^{241}Am and $^{90}Sr/^{90}Y$ of $\sim$10000 dpm activity concentration with α/β activity ratio 1

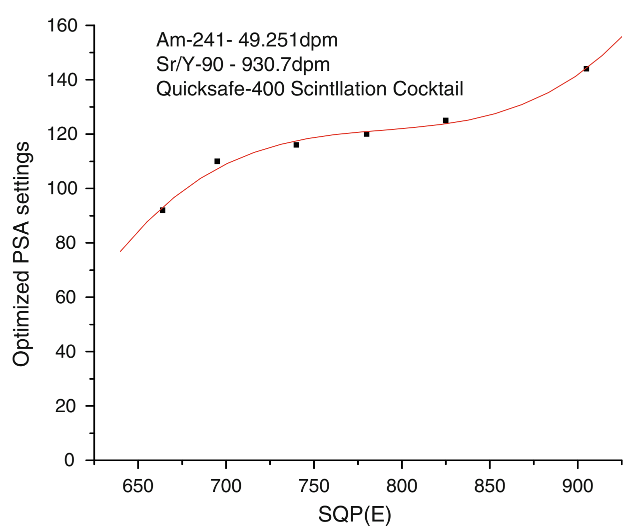

Fig. 3 Calibration plot prepared using ^{241}Am of 49.25 dpm and $^{90}Sr/^{90}Y$ of 930.7 dpm, in Quicksafe-400 scintillation cocktail with α/β activity concentration ratio of $\sim$1/20

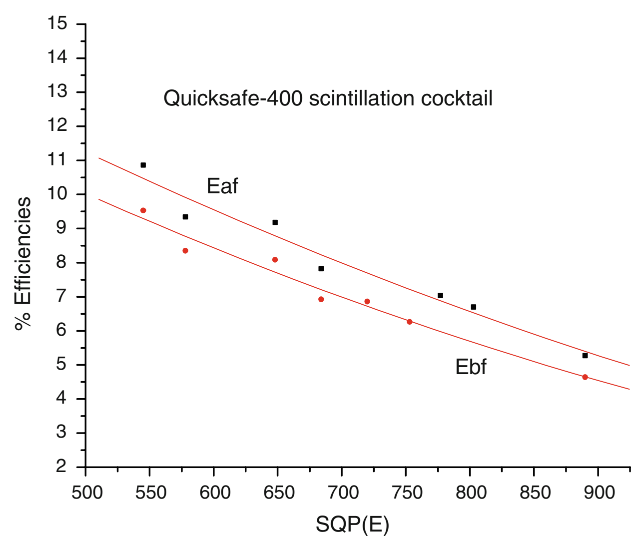

Fig. 5 Spillover efficiencies plotted against SQP(E) for ^{241}Am and $^{90}Sr/^{90}Y$ of $\sim 10^4$ dpm activity concentration with α/β activity ratio 1

These plots were used to determine PSA setting for a particular quench level. Quench correction curves as shown in Figs. 4 and 5 were plotted using detection (E_α and E_β) and spillover efficiencies ($E_{\alpha f}$ and $E_{\beta f}$) against SQP(E) and used to correct the measured activity. Detection efficiencies E_α and E_β decreased while spillover efficiencies $E_{\alpha f}$ and $E_{\beta f}$ increased with quench. It was also observed that higher degree of quench resulted in increase in the spillover of α event into β-MCA and β event into α-MCA. These results are consistent with those of Pujol, LI. and DeVol, T.A [5, 10].

Sample preparation

Test samples were prepared by adding the required amount (in g) of standard solutions of ^{241}Am and $^{90}Sr/^{90}Y$ to 12 mL of Quicksafe-400 (Zinsser Analytic) scintillation cocktail in polyethylene vials (Wheaton). The total sample and scintillation cocktail volume in the vial was maintained at 20 ml by adding 0.1 N acid carrier solution to the counting vial. Test samples were initially counted to know the quench level (SQP(E)) and then at subsequent optimized PSA setting that was obtained from the calibration plot. Quench studies were carried out using nitro-methane (Merck) as a chemical quencher.

Blank samples were prepared by adding 8 mL of 0.1 N acid carrier solution to 12 mL of Quicksafe-400 scintillation cocktail in a polyethylene counting vial to simulate sample preparation chemistry and counted along with each test sample. Prior to counting, quench level of blank sample was adjusted by adding Nitro methane so that the test sample and blank will have same degree of quench (identical SQP(*E*)).

Results and discussion

While analyzing the samples for gross alpha/beta activities, it is important to know the approximate activity level (or α/β activity ratio), source and chemical nature of the sample. These factors would lead to proper selection of calibration plot to be followed for the quantification of gross alpha and beta activities. Gomez Escobar et al. [11] described the anomalies observed in determining alpha activity with time and due to added chemicals using liquid scintillation calibration curve. The authors also compared accuracy and utility of quenching calibration curves with internal standard method and showed the incompetence of the constructed calibration curves for the test samples.

Performance of the 10^4 dpm, 25 dpm and $L_\alpha H_\beta$ calibration plots over a range of quench levels (550 < SQP(*E*) < 900) was tested for a number of spiked samples with different α/β activity ratios. Utility of these calibration plots was also checked for the range (minimum to maximum) of activity concentration values.

Gross alpha and beta activities calculation

Count rate observed in α and β-MCA is a function of both alpha and beta disintegrations plus their interference in β and α-MCA respectively. Equations 1 and 2 were used to calculate the gross alpha and beta activities [9]. Efficiency of alpha particles in alpha MCA is defined as E_α and its Spill-over efficiency in beta MCA is defined as $E_{\alpha f}$. Similarly efficiencies of beta particles in beta and alpha MCAs are defined as E_β and $E_{\beta f}$ respectively. These four efficiencies were used to determine the gross alpha (A_α) and gross beta (A_β) activities by solving the following equations:

$$Z_\alpha = A_\alpha E_\alpha + A_\beta E_{\beta f} \quad (1)$$

$$Z_\beta = A_\beta E_\beta + A_\alpha E_{\alpha f} \quad (2)$$

Equation 1 gives alpha count rate (Z_α) which is mainly because of alpha disintegrations ($A_\alpha E_\alpha$) in alpha MCA (SP12) and beta spillover ($A_\beta E_{\beta f}$) in the same MCA. Likewise Eq. 2 gives beta count rate (Z_β) that is a combination of both beta disintegrations ($A_\beta E_\beta$) and alpha spillover ($A_\alpha E_{\alpha f}$) in beta MCA (SP11).

Solving simultaneous Eqs. 1 and 2, we get

$$A_\alpha = \frac{Z_\alpha E_\beta - Z_\beta E_{\beta f}}{E_\alpha E_\beta - E_{\alpha f} E_{\beta f}} \quad \text{and} \quad A_\beta = \frac{Z_\beta E_\alpha - Z_\alpha E_{\alpha f}}{E_\alpha E_\beta - E_{\alpha f} E_{\beta f}}$$

where Z_α and Z_β are the count rates (cpm) of alpha and beta particles respectively.

Ratio of the difference between true dpm and calculated dpm to the true dpm gives the relative percentage deviation with respect to true activity concentration values of alpha and beta standards as derived from the equation.

$$\%deviation = \frac{(Truedpm - calculateddpm)}{Truedpm} \times 100$$

At the optimized PSA settings, alpha and beta activities were calculated along with percentage deviations with respect to the true activities (dpm). While deriving alpha and beta activities if the inaccuracies were found to be more than 10%, the test samples were counted at different PSA settings with ±10 unit variations from the optimized PSA setting. The difference between the PSA setting at which test sample showed minimum % deviation and the optimized PSA setting was used as a parameter to judge the practicability of the calibration plot. The minimum difference validates the efficacy of the calibration plot.

For alpha and beta events, full energy window corresponding to the entire spectrum (channels 1–1024) was utilized. Quantulus produces separate alpha and beta spectra in a single measurement. Figures 6, 7, 8 and 9 illustrate liquid scintillation spectra of discriminated ^{241}Am alphas and $^{90}Sr/^{90}Y$ betas in test samples with different quench levels and activity ratios.

Minimum detectable activity (MDA) values achieved for gross alpha and beta activities were 12.54 dpm/L (0.209 Bq/L) and 56.0 dpm/L (0.933 Bq/L) respectively for a counting time of 200 min. (SQP(*E*)—870).

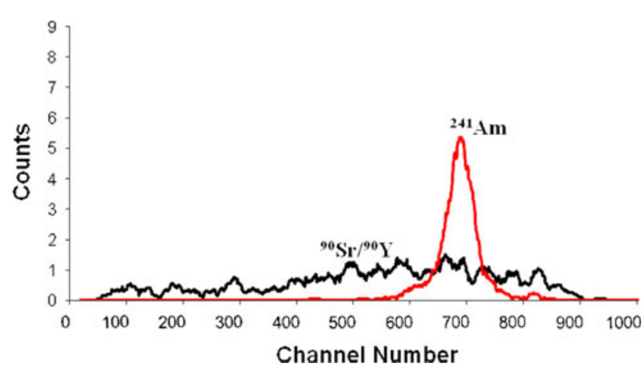

Fig. 6 Liquid scintillation spectra of discriminated alpha and beta in test sample (SQP(*E*)—835) spiked with ~10 dpm of ^{241}Am and $^{90}Sr/^{90}Y$ with alpha/beta activity concentration ratio 1

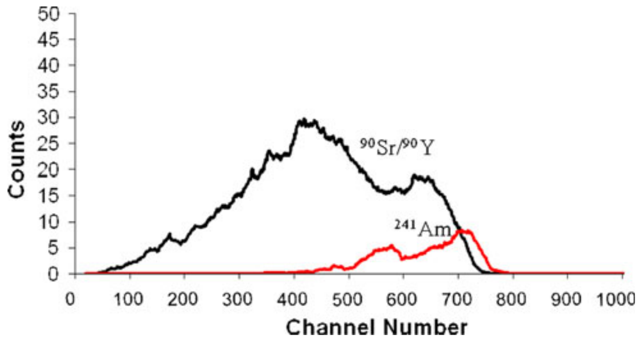

Fig. 7 Liquid scintillation spectra of discriminated alpha and beta in test sample (SQP(*E*)—685) spiked with ^{241}Am of 55 dpm and ^{90}Sr/^{90}Y of 2752 dpm with alpha/beta activity concentration ratio 1/50

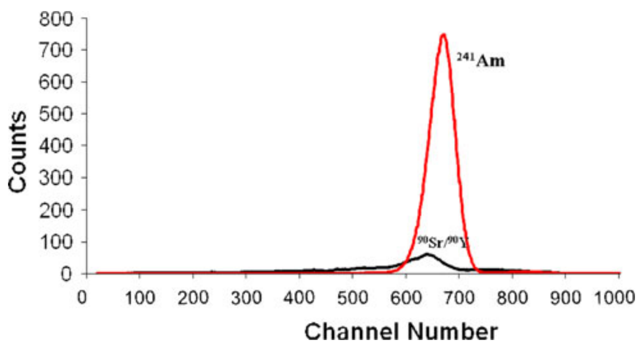

Fig. 8 Liquid scintillation spectra of discriminated alpha and beta in test sample (SQP(*E*)—817) spiked with ^{241}Am of 11072 dpm and ^{90}Sr/^{90}Y of 1561 dpm with alpha/beta activity concentration ratio 7

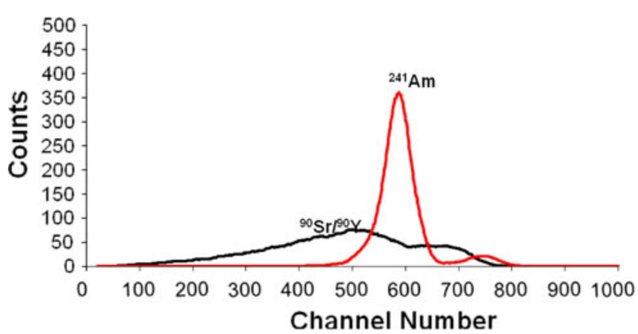

Fig. 9 Liquid scintillation spectra of discriminated alpha and beta in test sample (SQP(*E*)—719) spiked with ~14000 dpm of ^{241}Am and ^{90}Sr/^{90}Y with alpha/beta activity concentration ratio 1

Analysis of results obtained using ~10^4 dpm and ~25 dpm calibration plots

Practicability of calibration plot prepared employing ^{241}Am and ^{90}Sr/^{90}Y standards of activity concentration ~10^4 dpm (10^4 dpm calibration plot) was verified for the three sets of spiked samples as illustrated in Tables 1 and 2. First set comprises test samples with standardized ^{241}Am and ^{90}Sr/^{90}Y activity concentrations of equal value ($\alpha/\beta \sim 1$) in the range from 60 to 15000 dpm. Derived alpha and beta activities were within ±5.5% with at most 3 unit variations on the higher side (+3) of the optimized PSA settings.

Test samples ($L_\alpha H_\beta$) in second set were spiked with ^{241}Am of low activity concentration and ^{90}Sr/^{90}Y of high activity concentration in order to cover a range of α/β activity ratios from 1:2 to 1:20. In this study for α/β activity ratios 1:2 to 1:19.7, deviation was found to be within ±7% with at most 5 unit variations on the lower side (−5) of optimized PSA setting. In case of α/β activity ratio 1:21.5, inaccuracy observed was −32.6% with respect to alpha which is not acceptable. For α/β activity ratio 1:15, deviation with respect to alpha was found to be 12.6% because of low activity concentration of ^{241}Am (~32 dpm) in test sample. Hence it was concluded that 10^4dpm calibration plot worked satisfactory which resulted in deviation ≤±7% for a range of α/β activity ratios 1:2 to 1:20 with alpha activity concentration above 60 dpm. Test samples ($H_\alpha L_\beta$) in the third set were spiked with ^{241}Am of high activity concentration and ^{90}Sr/^{90}Y of low activity concentration to cover a range of α/β activity ratios from ~3:1 to ~20:1. For the test samples with activity ratios 3:1 to 19:1, derived alpha and beta activity concentrations were found to be within ±8% with −8 unit (maximum) variation from optimized PSA settings. In case of α/β activity ratio ~20:1, deviation of −21.3% was observed with respect to gross beta with −10 unit variation from optimized PSA setting, mainly due to low activity concentration (~55 dpm) of ^{90}Sr/^{90}Y.

To validate practicability of the 10^4 dpm and $L_\alpha L_\beta$ calibration plots, for the range of activity concentration level, test samples spiked with equal activity concentrations of ^{241}Am and ^{90}Sr/^{90}Y ($\alpha/\beta \sim 1$) covering an activity range of 8 to 200 dpm were analyzed using both the calibration plots as shown in Table 2. This exercise was necessary in order to find out, up to which activity concentration level these calibration plots provide agreeable (deviation < ±10%) results.

When the test samples spiked with equal activity concentrations of ^{241}Am and ^{90}Sr/^{90}Y ($\alpha/\beta \sim 1$) less than 60 dpm, were analyzed using $L_\alpha L_\beta$ calibration plot, calculated alpha and beta activities were within ±5.6% at the optimized PSA settings. Whereas, when the same samples were analyzed using 10^4 dpm calibration plot, ±4.3% deviation was observed at the cost of −8 unit variation (maximum) from optimized PSA setting. Test samples spiked with ^{241}Am and ^{90}Sr/^{90}Y ($\alpha/\beta \sim 1$) standards of activity concentrations above 60 dpm; however, when analyzed by 10^4 dpm calibration plot, derived alpha and beta activities were within ±5.5% as compared to ±8.5% deviation obtained with $L_\alpha L_\beta$ calibration plot. It is obvious from the above studies that $L_\alpha L_\beta$ calibration plot gave

Table 1 Validation results for different α:β activity ratios using ~10^4dpm calibration curve: calculated and true activity concentration values along with percentage deviation and PSA variation

α:β Activity ratio	α Weight fraction (g)[a]	β Weight fraction (g)[a]	True dpm α	True dpm β	Calculated dpm α	Calculated dpm β	% Devi. α	% Devi. β	± PSA vari
1:1	0.041	0.010	590.2[c]	618.3[e]	540.5 ± 5.2	618.3 ± 5.6	2.1	0.2	3
1:1	0.104	0.024	1482.6[c]	1549[e]	1410.6 ± 8.4	1527.9 ± 8.7	4.9	1.4	−1
1:1	0.306	0.071	4356.5[c]	4538.7[e]	4165.6 ± 14.8	4632.2 ± 8.9	4.4	−2.1	0
1:1	0.524	0.148	7472.7[c]	9453.6[e]	7434.6 ± 28.2	9488.9 ± 31.0	0.5	−0.4	1
1:1	1.035	0.228	14757[c]	14251[e]	14672.5 ± 39.9	14080.4 ± 37.8	0.6	3.0	0
1:2.2	0.306	0.148	4356.5[c]	9453.6[e]	4427 ± 21.73	9413.5 ± 31.0	−1.6	0.4	1
1:5.1	0.646	0.008	101.8[b]	522.72[e]	99.9 ± 1.5	553.87 ± 3.4	1.9	−6.0	−5
1:9.8	0.646	0.016	101.8[b]	1000.8[e]	95.2 ± 2.0	1020.5 ± 6.0	6.5	−2.0	−5
1:15.0	0.201	1.072	31.7[b]	481.28[d]	27.7 ± 1.0	478.0 ± 1.0	12.6	0.7	−5
1:17.5	0.646	0.028	101.8[b]	1778.5[e]	101.9 ± 2.3	1842.4 ± 7.7	−0.05	−3.6	−4
1:19.7	0.352	2.435	55.5[b]	1092.0[d]	52.6 ± 1.6	1028.4 ± 6.2	5.2	5.8	−3
1:21.5	0.646	0.034	101.8[b]	2192.9[e]	135 ± 2.8	2188.8 ± 9.5	−32.6	0.2	−3
2.8 :1	0.306	0.024	4356.5[c]	1549[e]	4284.8 ± 14.8	1537.7 ± 8.9	1.6	0.7	−2
5.1:1	0.020	0.121	279.4[c]	54.35[d]	281.1 ± 2.4	57.1 ± 1.2	−0.6	−5.1	−7
7.1:1	0.777	0.025	11072[c]	1561.4[e]	10835.4 ± 34.0	1607.1 ± 13.5	2.1	−2.9	−8
10:1	1.527	0.034	21769[c]	2186.2[e]	21515.3 ± 34.3	2346.2 ± 15.7	1.2	−7.3	0
10.7:1	0.041	0.121	578.8[c]	54.35[d]	581.4 ± 4.5	50.1 ± 1.5	−0.5	7.8	−8
16.5:1	0.063	0.121	893.8[c]	54.35[d]	914.1 ± 5.6	50.3 ± 1.7	−2.3	7.4	−5
19.1:1	0.777	0.009	11072[c]	580.1[e]	10448 ± 33.0	604.6 ± 9.0	5.6	−4.2	−2
20.1:1	0.077	0.121	1093.4[c]	54.35[d]	1172.8 ± 6.8	65.9 ± 1.7	−2.3	−21.3	−10

[a] Weight fractions are rounded to three decimals

[b] ^{241}Am—157.52 dpm/mL

[c] ^{241}Am—14255.2 dpm/mL

[d] ^{90}Sr/^{90}Y—449.15 dpm/mL

[e] ^{90}Sr/^{90}Y—63746.7 dpm/mL

Table 2 Comparison of results obtained by 10^4 dpm and $L_\alpha L_\beta$ (~25 dpm) calibration plots for test samples with α/β activity ratio ~1

Samples analyzed by	α Weight fraction (g)	β Weight fraction (g)	True dpm α	True dpm β	Calculated dpm α	Calculated dpm β	% Devi. α	% Devi. β	± PSA vari.
10^4 dpm Calibration plot	0.053	0.021	8.4[a]	9.3[b]	8.6 ± 0.1	8.9 ± 0.2	−2.4	4.3	−8
	0.171	0.075	26.9 [a]	33.6[b]	25.9 ± 0.4	32.9 ± 0.5	3.7	2.1	−6
	0.332	0.130	52.3[a]	58.6[b]	51.2 ± 0.5	58.4 ± 0.6	2.1	0.4	−8
	0.437	0.161	68.9[a]	72.4[b]	72.7 ± 0.6	69.3 ± 0.6	−5.5	4.3	−1
	0.611	0.241	96.2[a]	108.0[b]	99.0 ± 0.7	103.0 ± 0.8	−2.9	4.6	−1
	0.820	0.307	129.1[a]	137.7[b]	132.0 ± 0.8	134.8 ± 0.9	−2.2	2.1	2
	1.272	0.452	200.4[a]	203.2[b]	209.4 ± 1.0	201.7 ± 1.0	−4.5	0.8	0
$L_\alpha L_\beta$ Calibration plot	0.053	0.021	8.4[a]	9.3[b]	8.5 ± 0.2	9.2 ± 0.3	−1.2	1.1	0
	0.171	0.075	26.9[a]	33.6[b]	25.4 ± 0.4	32.6 ± 0.5	5.6	3.0	0
	0.332	0.130	52.3[a]	58.6[b]	50.7 ± 0.5	57.8 ± 0.6	3.0	1.4	0
	0.437	0.161	68.9[a]	72.4[b]	68.3 ± 0.6	67.4 ± 0.6	0.9	6.9	−2
	0.611	0.241	96.2[a]	108.0[b]	93.2 ± 0.7	98.9 ± 0.8	3.1	8.5	2
	0.820	0.307	129.1[a]	137.7[b]	130.7 ± 0.8	126.7 ± 0.9	−1.2	8.0	2
	1.272	0.452	200.4[a]	203.2[b]	201.0 ± 1.0	190.0 ± 1.0	−0.3	6.5	0

[a] ^{241}Am—157.52 dpm/mL

[b] ^{90}Sr/^{90}Y—449.15 dpm/mL

Table 3 Calculated and true activity concentrations along with percentage deviation and PSA variation for test samples containing 31.7[a] dpm of ^{241}Am and different activity concentrations of ^{90}Sr/^{90}Y

α:β Activity ratio	β Weight fraction (g)	True dpm β	Calculated dpm α	Calculated dpm β	% Devi. α	% Devi. β	± PSA vari.
1:5	0.358	160.9[b]	33.0 ± 1.1	157.8 ± 2.4	−4.1	1.9	0
1:10	0.713	320.2[b]	32.1 ± 1.1	307.1 ± 3.3	−1.3	4.1	0
1:15	1.0716	481.3[b]	30.9 ± 1.2	477.2 ± 4.1	2.5	0.9	2
1:20	1.4213	638.4[b]	29.1 ± 1.3	636.7 ± 4.8	8.2	0.3	3
1:25	0.0125	797.3[c]	39.7 ± 1.5	777.0 ± 5.3	−25.2	2.5	3

Alpha weight fraction: 0.2012 g

[a] ^{241}Am—157.52 dpm/mL

[b] ^{90}Sr/^{90}Y—449.15 dpm/mL

[c] ^{90}Sr/^{90}Y—63746.7 dpm/mL

precise results as compared to 10^4 dpm calibration plot for samples containing ^{241}Am and ^{90}Sr/^{90}Y ($\alpha/\beta \sim 1$) less than 60 dpm.

Analysis of results obtained by $L_\alpha H_\beta$ calibration plot

Almost all real samples such as drinking water, environmental and effluent samples show high beta and low alpha activity concentrations [12]. To simulate these activity levels, different test samples were spiked with ^{241}Am of low activity concentration (of range 31.7–331.1 dpm) and ^{90}Sr/^{90}Y of high activity concentration (of range 160.9–5514.6 dpm). Practicability of $L_\alpha H_\beta$ calibration plot was studied for these test samples that were grouped in three categories depending on their alpha activity concentration viz. 31.7, 55.5 and 145.7 dpm respectively. Test samples in each category were spiked with the same activity concentration of ^{241}Am and different activity concentrations of ^{90}Sr/^{90}Y in order to cover a range of α/β activity ratios from 1:5 to 1:50. These activity proportions were considered so as to cover most environmental situations [13].

For the first category of test samples as illustrated in Table 3, where alpha activity concentration was lowest (31.7 dpm), results were found to be in good agreement with the true alpha and beta activity concentrations for α/β activity ratios 1:5–1:15. Deviations observed for these activity ratios were within ±4.1% with merely 2 unit variations from optimized PSA setting. For the activity ratio 1:20 (α/β), deviation with respect to alpha increased to ∼8%, higher deviation which amounts to −25.2% for 1:25(α/β) activity ratio was insignificant and hence rejected.

As illustrated in Table 4, test samples spiked with 55.5 dpm of ^{241}Am with different activity concentrations of ^{90}Sr/^{90}Y, were analyzed using $L_\alpha H_\beta$ calibration plot. For test samples with α/β activity ratios ∼1:10 to 1:25, inaccuracy of 5.2% was observed in deriving alpha and beta activities with merely 1 unit variation from the optimized PSA setting. Test sample with α/β activity ratio ∼1:30, showed deviation of 6.3% with respect to beta with −5 unit variation from the optimized PSA setting. For α/β activity ratios 1:35, 1:43.1 and 1:50 where deviations observed

Table 4 Calculated and true activity concentrations along with percentage deviation and PSA variation for test samples containing 55.5[a] dpm of ^{241}Am and different activity concentrations of ^{90}Sr/^{90}Y

α:β Activity ratio	β Weight fraction (g)	True dpm β	Calculated dpm α	Calculated dpm β	% Devi. α	% Devi. β	± PSA vari.
1:9.5	1.1711	526.0[b]	54.0 ± 1.4	522.6 ± 4.3	2.7	0.6	0
1:15.1	1.8711	838.7[b]	55.0 ± 1.6	820.6 ± 5.4	0.9	2.2	1
1:19.7	2.4313	1092.0[b]	53.9 ± 2.4	1068.0 ± 8.7	3.0	2.2	1
1:25	3.0916	1388.6[b]	52.6 ± 2.3	1328.9 ± 9.8	5.2	4.3	1
1:30.4	3.7599	1688.8[b]	55.5 ± 3.1	1581.9 ± 10.8	0	6.3	−5
1:35	4.3237	1942.0[b]	39.3 ± 3.1	1864.5 ± 11.7	29.1	4.0	−6
1:43.1	5.3250	2391.7[b]	50.7 ± 3.4	2113.4 ± 12.4	8.6	11.6	−4
1:49.6	6.1270	2752.0[b]	44.0 ± 3.5	2497.7 ± 13.5	20.7	9.2	−5

Alpha weight fraction: 0.3523 g

[a] ^{241}Am—157.52 dpm/mL

[b] ^{90}Sr/^{90}Y—449.15 dpm/mL

Table 5 Determination of gross alpha/beta activities by $L_\alpha H_\beta$ calibration plot for test samples containing 145.7[a] dpm of ^{241}Am along with different activity concentrations of ^{90}Sr/^{90}Y

α:β Activity ratio	β Weight fraction (g)	True dpm β	Calculated dpm α	Calculated dpm β	% Devi. α	% Devi. β	± PSA vari.
1:6.4	0.0125	797.3[b]	140.7 ± 3.1	779.3 ± 7.6	3.4	2.3	4
1:10.9	0.0211	1345.5[b]	138.5 ± 3.4	1367.2 ± 9.9	4.9	−1.6	−2
1:15.9	0.0308	1960.8[b]	152.2 ± 3.7	1960.8 ± 12.0	−4.5	0	−4
1:20.8	0.0404	2575.8[b]	139.6 ± 4.1	2508.8 ± 13.7	4.2	2.6	−6
1:25.4	0.0493	3143.2[b]	148.6 ± 4.6	3111.6 ± 15.1	−2.0	1.0	4
1:31	0.0602	3838.0[b]	137.4 ± 4.7	3740.4 ± 16.8	5.7	2.5	5
1:36.2	0.0702	4475.5[b]	135.2 ± 5.0	4332.3 ± 18.1	7.2	3.2	6
1:41.1	0.0800	5093.8[b]	137.7 ± 5.4	5060.9 ± 19.4	5.5	0.7	0
1:44.5	0.0866	5514.6[b]	154.0 ± 5.6	5432.6 ± 20.0	−5.7	1.5	5

Alpha weight fraction: 0.0102[a]g

[a] ^{241}Am—14255.2 dpm/mL

[b] ^{90}Sr/^{90}Y—63746.7 dpm/mL

were more than 10%, highlighted the non-reliability of $L_\alpha H_\beta$ calibration plot for these activity ratios.

Test samples spiked with 145.7 dpm of ^{241}Am and different activity concentrations of ^{90}Sr/^{90}Y with a range of α/β activity ratios ~1:5 to ~1:45 were also studied using $L_\alpha H_\beta$ calibration plot as illustrated in Table 5. Inaccuracies observed in estimating alpha and beta activities were within ±7.2% with ±6 unit variation from the optimized PSA setting. This study emphasizes the usefulness of the above calibration plot for a wide range of α/β activity proportions with alpha activity concentration ~150 dpm.

The test samples with alpha/beta activity ratios such as 1:5, 1:10, 1:15, 1:18 and 1:20 were analyzed using ~10^4 dpm as well as $L_\alpha H_\beta$ calibration plots and the results were compared as shown in Table 6. Inaccuracies in estimating respective alpha and beta activities in these test samples were found to be within ±6.5% (except 1:15 (α:β) activity ratio) with ±6 unit variation from optimized PSA setting when analyzed by 10^4dpm calibration plot. This is in contrast to $L_\alpha H_\beta$ calibration plot where ±5% deviation (except 1:18 (α:β) activity ratio) with merely ±2 unit variation from optimized PSA setting was observed. The test sample with α/β activity ratio 1:18 and alpha activity concentration 331.1 dpm, when analyzed by $L_\alpha H_\beta$ calibration plot, deviation was found to be 28.7% with respect to alpha. On the contrary when the same test sample was analyzed by 10^4 dpm calibration plot, the results were found to be within 6% which signifies the efficacy of 10^4 dpm calibration plot with alpha activity more than 300 dpm.

Practicability of the 10^4 dpm and $L_\alpha H_\beta$ calibration plots was studied for a range of alpha activity concentrations as illustrated in Table 7. Table 7 confirms the usefulness of $L_\alpha H_\beta$ calibration plot over 10^4 dpm calibration plot for the wide range of α/β activity ratios with the alpha activity concentration less than 300 dpm whereas 10^4 dpm calibration plot worked satisfactory above 300 dpm.

Table 6 Comparison of results obtained by ~10^4dpm and $L_\alpha H_\beta$ calibration plots for test samples with different α:β activity ratios

Samples analyzed by	α:β Activity ratios	True dpm α	True dpm β	Calculated dpm α	Calculated dpm β	% Devi. α	% Devi. β	± PSA vari.
10^4 dpm Calibration plot	1:5	101.8	522.7	99.9 ± 1.5	553.9 ± 3.4	1.9	6.0	−5
	1:10	101.8	1000.8	95.2 ± 2.0	1020.5 ± 6.0	6.5	2.0	−5
	1:15	31.7	481.3	27.7 ± 1.0	478.0 ± 1.0	12.6	0.7	−5
	1:18	331.1	5514.6	312.6 ± 5.0	5579.9 ± 17.4	5.6	1.2	6
	1:20	55.5	1092.0	52.6 ± 1.6	1028.4 ± 6.2	5.2	5.8	−3
$L_\alpha H_\beta$ Calibration plot	1:5	31.7	160.9	33.0 ± 1.1	157.8 ± 2.4	−4.1	1.9	0
	1:10	145.7	1345.5	138.5 ± 3.4	1367.2 ± 9.9	4.9	−1.6	−2
	1:15	31.7	481.3	30.9 ± 1.2	477.2 ± 4.1	2.5	0.9	2
	1:18	331.1	5514.6	236.1 ± 6.1	5607.4 ± 15.7	28.7	1.7	1
	1:20	55.5	1092.0	53.9 ± 2.4	1068.0 ± 8.7	3.0	2.2	1

Table 7 Performance validation of $\sim 10^4$dpm and $L_\alpha H_\beta$ calibration plots with respect to alpha activity concentration in $L_\alpha H_\beta$ test samples

Samples analyzed by	α Activity (dpm)	Maximum % devi. with respect to alpha	Range of $\alpha:\beta$ activity ratios with acceptable deviation	± PSA vari.
10^4 dpm Calibration plot	~30	12.6	1:15	−5
	~50	5.2	1:20	−3
	~100	6.5	1:5–1:18	−5
	>300	5.6	1:18	6
$L_\alpha H_\beta$ Calibration plot	~30	8.2	1:5–1:20	3
	~50	5.2	1:10–1: 25	1
	~150	7.2	1:6–1:45	6
	>300	28.7	1:18	1

Conclusion

Liquid scintillation counting technique offers simultaneous gross alpha and gross beta measurement with ~100% counting efficiency. In conclusion, all the three calibration plots viz. 10^4 dpm, $L_\alpha L_\beta$ and $L_\alpha H_\beta$ have certain limitations over the activity concentration level and α/β activity proportions. These limitations should be taken into account for the accurate measurement of gross alpha and gross beta activities. When practicability of these three calibration plots were compared, it was found that the choice of proper calibration plot plays a vital role in determining gross alpha and gross beta activities in a given sample. The validation trials with artificially spiked samples confirmed that the calibration plots compensate for varying quench in sample.

References

1. Outola I, Nour S, Kurosaki H, Inn K, La Rosa J, Lucas L, Volkovitsky P, Koepenick K (2008) Investigation of radioactivity in selected drinking water samples from Maryland. J Radioanal Nucl Chem 277(1):155–159
2. Kaihola L (May 28–30, 1990) Ultra low background liquid scintillation spectrometry of alpha particles, presented at the "International Seminar on Low-level Counting in Environmental Radioactivity Monitoring", Estonian Academy of Sciences, Talling
3. Kleinschmidt RI (2004) Gross alpha and beta activity analysis in water—a routine laboratory method using liquid scintillation analysis. Appl Radiat Isot 61:333–338
4. Horrocks DL (1970) Pulse shape discrimination with organic liquid scintillator solutions. Appl Spectrosc 24(4)
5. DeVol TA, Theisen CD, DiPrete DP (2007) Effect of quench on alpha/beta pulse shape discrimination of liquid scintillation cocktails. Health Phys 92(supplement 2):S105–S111
6. Wong CT, Soliman VM, Perera SK (2005) Gross alpha/beta analyses in water by liquid scintillation counting. J Radioanal Nucl Chem 264(2):357–363
7. Grau malonda A (1982) Evaluation of counting efficiency in liquid scintillation counting of pure beta ray emitters. Appl Radiat Isot 33:249–253
8. Sanchez-Cabeza JA, Pujol LI, Merino J, Molero J, Vidal-Quadras A, Schell WR, Mitchell PI (1993) Optimization and calibration of a low background liquid scintillation counter for the simultaneous determination of alpha and beta emitters in aqueous samples. In: Noakes JE, Schonhofer F, Polach HA (eds) Advances in liquid scintillation spectrometry. Radiocarbon, Tucson, pp 43–50
9. L'Annunziata MF (2003) Handbook of radioactivity analysis, 2nd edn. Academic Press, San Diego, pp 445–455
10. Pujol LI, Sanchez-Cabeza JA (1997) Role of quenching on alpha/beta separation in liquid scintillation counting for several high capacity cocktails. Anal 122:383–385
11. Gomez Escobar V, Vera Tome F, Lozano JC (1999) Extractive scintillators for alpha liquid scintillation counting: anomalies in quenching evaluation. J Radioanal Nucl Chem 240(3):913–915
12. Davila rangel JI, Lopez del Rio H, Mireles Garcia F, Quirino Tor LL, Villalba ML, Colmenero Sujo L, Montero Cabrera ME (2002) Radioactivity in bottled waters sold in Mexico. Appl Radiat Isot 56:931–936
13. Sanchez-Cabeza JA, Pujol LI (1995) A rapid method for the simultaneous determination of gross alpha and beta activities in water samples using a low background liquid scintillation counter. Health Phys 68(5):674–682